PREDICTION OF CREEP CRACK INITIATION USING A DAMAGE-BASED APPROACH

C. M. Davies, M. Yatomi, N. P. O'Dowd, K. M. Nikbin
Department of Mechanical Engineering, Imperial College London, UK

ABSTRACT

This paper presents a numerical study of creep crack initiation and growth in a fracture mechanics specimen. Creep data have been collected on uniaxial specimens of carbon-manganese steel at 360°C and Type 316H stainless steel at 550°C. The constitutive behaviour of the steel is described by a power law creep model and the deformation of the specimen is modelled using the finite element method. Elastic-creep and elasti-plastic-creep analyses are performed to predict crack extension under plane stress and plane strain conditions. Crack initiation and propagation is predicted based on the accumulation of ductile damage associated with void growth and coalescence. The results from the simulations are compared to experimental data. The sensitivity of the predictions to mesh size is high and merits further investigation.

1 INTRODUCTION

Many components used in power generation plants are continually exposed to high temperatures and crack initiation and growth can occur within the high temperature regime. Safe and accurate methods to predict creep crack initiation (CCI) and growth (CCG) are therefore required in order to assess the reliability of such components. With advances in finite element (FE) methods, more complex models can be applied in the study of CCI and CCG where simple analytical solutions or approximate methods are no longer applicable. In this work creep crack initiation and growth is examined using FE analysis and the results are compared with experimental data.

In previous studies, e.g. Hayhurst *et al.* [1], FE calculations using a Kachanov [2] type damage variable to account for the evolution of creep damage within a material have been performed and special procedures have been used to remove elements within the mesh which have reached a critical level of damage. The loss of load bearing capacity due to creep damage within the element is thus accounted for. However, the removal of elements may not accurately model the situation where a sharp crack is growing within a creeping material. In this work therefore an alternative approach is adopted whereby nodes ahead of the crack tip are released when the damage reaches a critical value. A similar node-release approach to model crack growth under creep conditions has been employed in recent work by Zao *et al.* [3] and Saxena *et al.* [4], however in these models the crack growth rate has been assumed *a priori*, based on experimental data, and has not been determined within the analysis. Therefore the approach cannot be used for the prediction of CCG.

2 MATERIAL DATA AND MODELLING

2.1 Uniaxial Creep Properties

The material properties have been obtained from uniaxial tensile and creep tests from Maskell *et al*. [5] for a high carbon-manganese (C-Mn) at 360°C and from Bettinson [6] for 316H at 550°C. In general, creep deformation can be considered to be composed of three regimes, namely primary, secondary and tertiary creep regimes. The use of an average creep rate obtained directly from creep rupture data has been proposed to account for all three stages of creep. This average creep rate, $\dot{\varepsilon}_A$, is defined by

$$\dot{\varepsilon}_A = \frac{\varepsilon_f}{t_r} = \dot{\varepsilon}_o \left(\frac{\sigma}{\sigma_0} \right)^n = A\sigma^n , \tag{1}$$

where ε_f is the uniaxial failure strain, t_r is the time to rupture and σ is the applied stress. The variables, σ_0, A and n in eqn (1) are generally taken as temperature dependent material constants. For these materials ε_f has been found to be relatively independent of the applied stress magnitude. Details of the relevant material properties are given in Table 1, in which the units of A and n are for stress in MPa and time in hours.

Material	Temperature (^{o}C)	Young's Modulus (GPa)	σ_y (MPa)	A	n	ε_f
C-Mn Steel	360	190	240	1.78×10^{-32}	10.00	18%
Type 316H Stainless Steel	550	140	170	7.227×10^{-32}	10.62	21%

Table 1: Material properties for C-Mn Steel and Type 316H stainless steel.

3 FINITE ELEMENT MODELLING

3.1 Damage Accumulation

In this study the creep ductility exhaustion approach is used to account for the accumulation of creep damage following the approach by Yatomi *et al* [7]. The damage parameter, ω, is defined such that $0 \le \omega \le 1$ and failure occurs when ω approaches 1. The rate of damage accumulation, $\dot{\omega}$, is related to the equivalent creep strain rate by the relationship,

$$\dot{\omega} = \frac{\dot{\varepsilon}^c}{\varepsilon_f^*} , \tag{2}$$

and the total damage at any instant is the integral of the damage rate in eqn (2) up to that time

$$\omega = \int_0^t \dot{\omega}\, dt . \tag{3}$$

Thus, failure occurs in the vicinity of the crack tip when the local accumulated strain reaches the local (multiaxial) creep ductility, ε_f^*, which may be obtained for the material under study from the Cocks and Ashby [8] model. The model describes the ratio of the multiaxial to uniaxial failure strain, $\varepsilon_f^* / \varepsilon_f$, as

$$\frac{\varepsilon_f^*}{\varepsilon_f} = sinh\left[\frac{2}{3}\left(\frac{n-1/2}{n+1/2} \right) \right] \Big/ sinh\left[2\left(\frac{n-1/2}{n+1/2} \right) \frac{\sigma_m}{\sigma_e} \right] , \tag{4}$$

where σ_m/σ_e is the ratio between the mean (hydrostatic) stress and equivalent (von Mises) stress, which is often referred to as the triaxiality.

3.2 Elastic Plastic and Creep Strains

Calculations are performed using elastic-creep and elastic-plastic-creep behaviour. In the latter case the plastic strains are understood to be independent of strain rate giving the total strain as

$$\varepsilon = \varepsilon^{el} + \varepsilon^{pl} + \varepsilon^{cr} , \tag{5}$$

where ε^{el}, ε^{pl} and ε^{cr} are elastic, plastic and creep strains respectively.

3.3 Finite Element Model

A two dimensional FE model of a CT specimen with W = 25 mm, B = 12.5 mm and a/W = 0.45 is examined. Different meshes for the CT specimen are used in order to examine the influence of mesh size. For the coarse mesh in Figure 1 (a) the mesh size at the crack tip is 0.25 mm, while for the fine mesh in Figure 1 (b) the mesh size at the crack tip is approximately 0.0154 mm, which is similar to the grain size of the C-Mn steels examined. A medium mesh is also used that is similar to the fine mesh but has a mesh size at the crack tip of approximately 0.0625 mm, which is more comparable with the grain size of Type 316H steel. A typical coarse, medium and fine mesh contains 602, 2997 and 8461 four noded elements, respectively. Finite element analyses were conducted using ABAQUS [9].

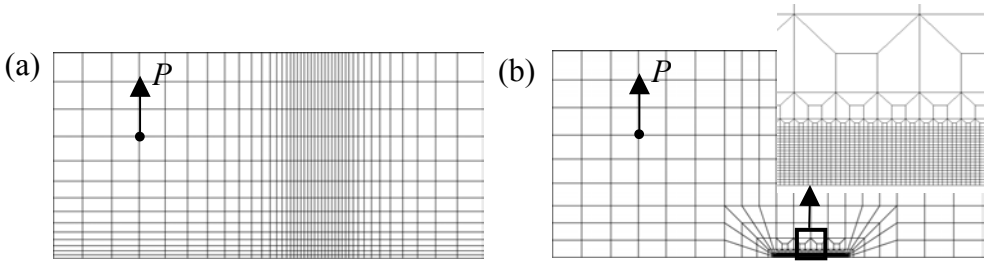

Figure 1: FE mesh for CCG analysis of CT specimen (a) coarse mesh and (b) fine mesh.

Crack extension is predicted by the crack tip node being released when damage, ω, as derived from eqns (2) and (3) approaches unity at two integration points in the element directly ahead of the crack tip. As a result the crack propagates through the mesh along the axis of symmetry. It is assumed that the crack grows in the plane of the initial crack front, *i.e.* along the symmetry plane. The model therefore assumes a flat crack front, rather than multiple microscopic cracks linking up ahead of the main crack front, which is generally observed under creep crack growth conditions, *e.g.* Bettinson [6]. A user subroutine (multi-point constraint, MPC), which allows the user to alter nodal constraints during the analysis, was used to release the nodes. Within this subroutine, the displacement at a node is held fixed until the node is to be released and, subsequent to the release, the node is allowed to move independently. In the crack growth analysis the maximum extent of crack growth is determined by the mesh design (crack grows through a region of uniform sized elements as shown in the inset to Figure 1(b)). With this mesh design the maximum amount of crack growth is approximately 3.75 mm (*i.e.* 0.33a) for the three meshes.

4 FINITE ELEMENT RESULTS

The effect of mesh size and crack tip plasticity on the predictions from the node-release model is examined. The predicted increase in crack length with time for each analysis is shown in Figure 2 for C-Mn and in Figure 3 for 316H. The data for the C-Mn steel has previously been presented by Yatomi *et al* [10]. Analyses have been carried out under plane stress and plane strain conditions with and without plastic deformation. The load, P, applied to the specimen was 9 kN for the C-Mn material and 8.5 kN for the 316H material. Results are presented for the coarse and fine mesh for the two materials. For the coarse mesh, the first node released is at a distance of 0.25 mm from the crack tip. Therefore, the FE results are extrapolated back to the initial crack length (Δa = 0) using the slope of the predicted curve at the first increment of crack growth.

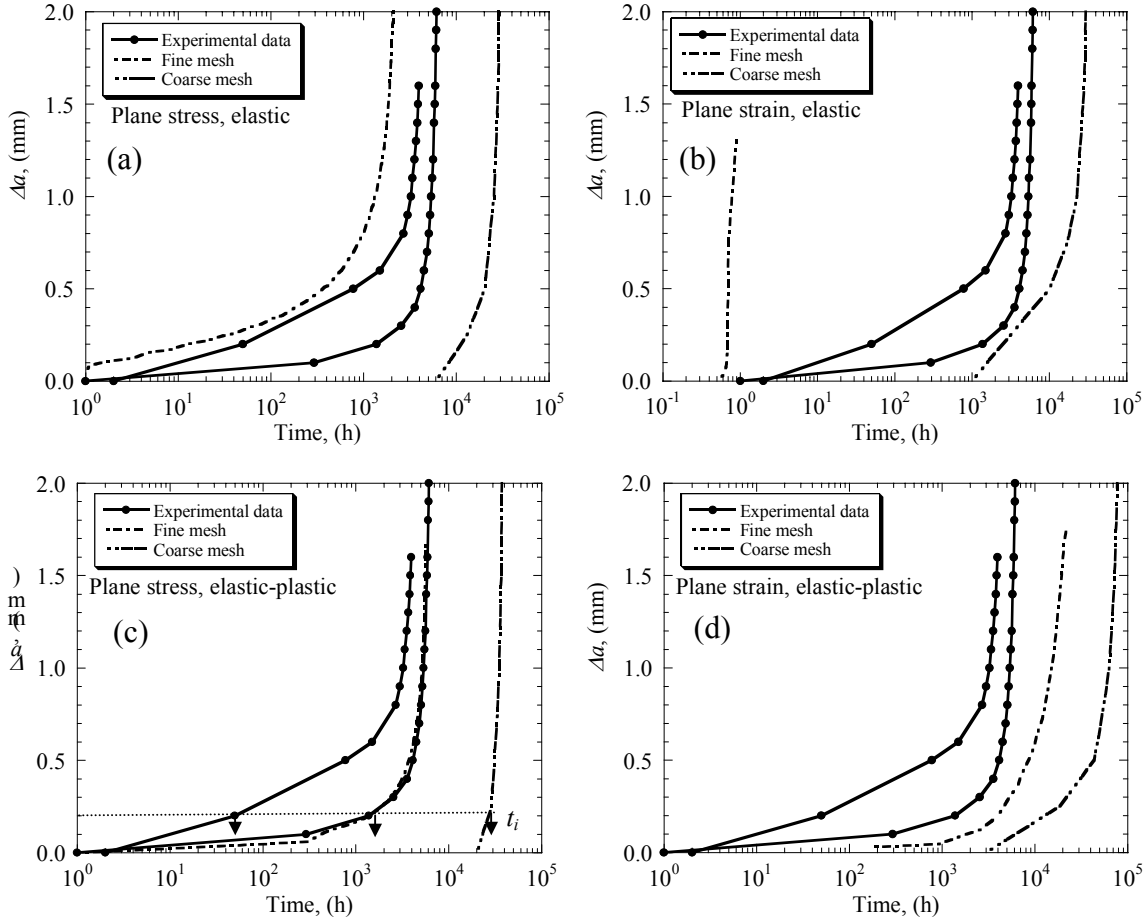

Figure 2: Effect of mesh size, out of plane stress state (plane stress/plane strain) and material behaviour on predicted CCI and CCG in C-Mn.

It is found that releasing a node, *i.e.* switching off an MPC, can cause a numerical instability equilibrium, which may lead to convergence problems. This numerical difficulty is encountered most severely in the elastic-plastic-creep analyses for 316H material, causing the analysis to terminate. As the mesh is refined, numerical difficulties occur sooner in the analyses. Consequently, for the fine mesh, only one data point is obtained in the plane stress analysis and no data is obtained under conditions of plane strain, as seen in Figures 3 (c) and (d), respectively. Hence, results from the medium mesh are also included in these two figures. It is seen that in all cases a reduction in mesh size leads to an increase in the predicted crack growth rate for both plane stress and plane strain conditions. (Note that the difference in mesh size between the coarse and fine mesh is more than an order of magnitude). Thus, using the nodal release method does not eliminate the effect of mesh size on crack growth predictions. It is seen however, that the use of the fine mesh produces a more conservative result—the predicted crack growth rates for the fine mesh in Figure 2 (a) and (b) are higher than the experimental values.

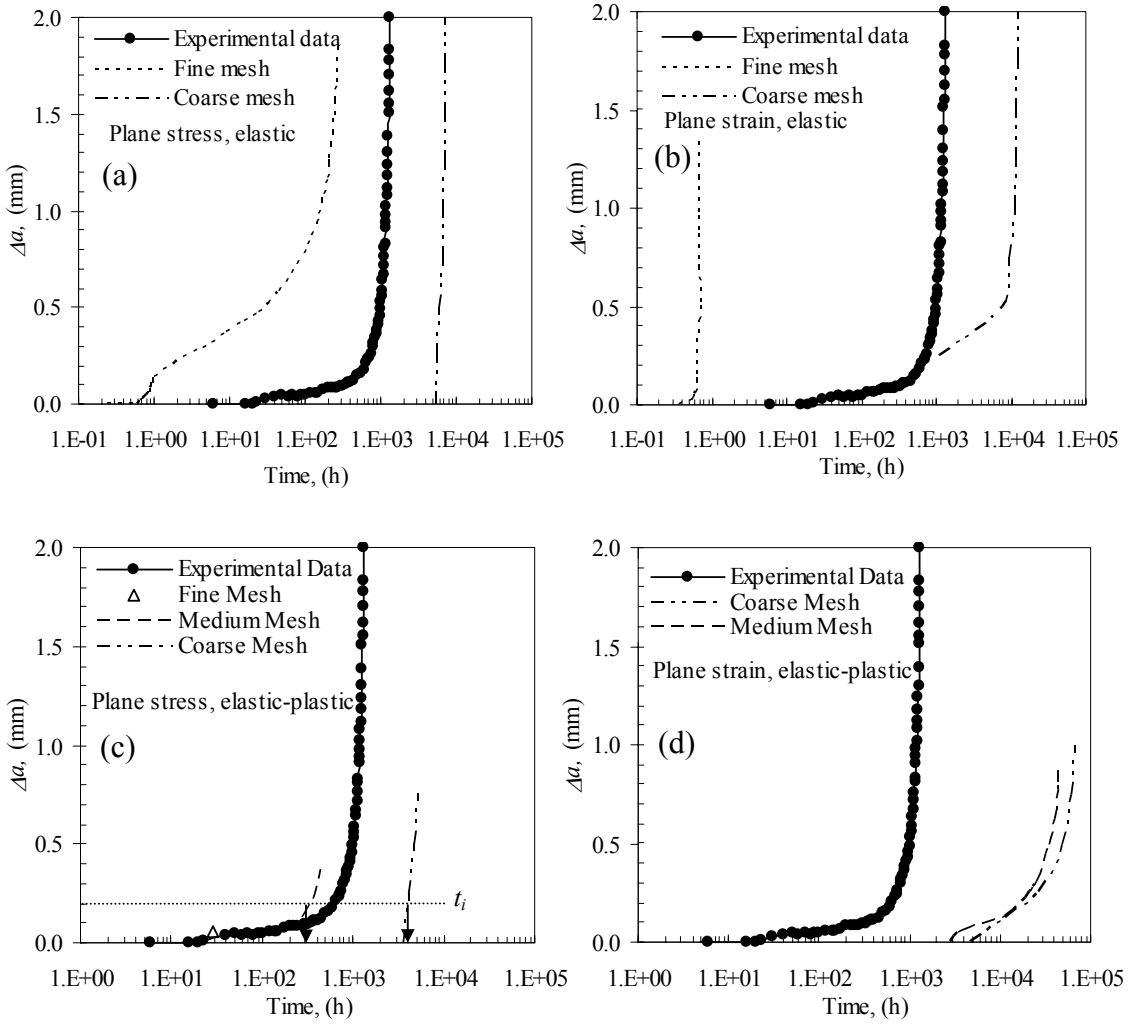

Figure 3: Effect of mesh size, out of plane stress state (plane stress/plane strain) and material behaviour on predicted CCI and CCG on predicted CCG in Type 316H stainless steel.

The effects of plastic deformation are examined in Figures 2 and 3 (c) and (d). It can be seen that the inclusion of crack tip plasticity leads to a decrease in the amount of crack growth at the same load, particularly for the fine mesh analysis. This is because the crack tip stresses at short times are reduced due to plastic deformation and the creep strain rates are therefore also reduced. It has also been found that under plane strain conditions the crack tip triaxiality is also reduced when plasticity is included. Since plastic strains do not contribute to creep damage (see eqn (2)) the overall effect is a reduction in the amount of crack growth for the same applied load. It is also clear from Figure 2 and 3 that the effect of plasticity is less significant for the coarse mesh—for the coarse mesh the stress levels at the crack tip are not sufficient to lead to significant amounts of plastic strain. It can be seen in Figures 2 and 3 that the mesh size effect is more significant for the

elastic analysis than the elastic-plastic analysis. This is to be expected, as plastic deformation will reduce the high stress concentration at the sharp crack tip in the fine mesh. Thus the inclusion of plastic strains tends to mitigate the effect of mesh size and reduce the conservatism of the fine mesh analysis leading (in this case) to an under prediction of the crack growth rate if plane strain conditions are assumed. However, the excellent agreement between the plane stress elastic-plastic model and the experimental data Figure 2(c)) is noted. This analysis predicts an initiation time of approx. 1500 hours (based on a crack growth of 0.2 mm) while the measured initiation time lies between 40 and 1500 hours. Studies on the 316H material are ongoing.

5 DISCUSSION AND CONCLUSIONS

This paper presents methods for predicting creep crack growth in a CT specimen, using a damage variable to quantify time dependent crack tip degradation. The materials examined are a carbon-manganese steel at a test temperature of 360 ºC and 316H stainless steel at 550^{o}C. A power law creep model is used to describe the constitutive behaviour of the steel and both plane stress and plane strain conditions are examined using the finite element method. The effect of mesh size, crack tip plasticity on the creep crack growth rate were examined and found to have a stronger influence under plane strain conditions than under plane stress conditions.

6 REFERENCES

[1] Hayhurst, D.R., Brown, P.R. and Morrison, C.J., "The role of continuum damage in creep crack growth", Phil. Trans. R. Soc. Lond. A, **311**, 131–158, 1984.

[2] Kachanov, L.M., "Introduction to Continuum Damage Mechanics", Kluwer Academic Publishers, Dordrecht, 1986.

[3] Zao, L.G., Tong, J., Byrne, J., "Finite element simulation of creep-crack growth in a nickel base super alloy", Eng. Frac. Mech., **68**, 1157–1170, 2001.

[4] Saxena, A., Hall, D.E., McDowell, D.L., "Assessment of deflection rate partitioning for analysing creep crack growth data", Eng. Frac. Mech., **62**, 111–122, 1999.

[5] Maskell, R. V., Fleming, A., Crawford, P. J. and Buchanan, L. W., "Creep crack growth in internally pressurised tubes", J. Materials at High Temperature, **15(3/4)** 151–158, 1998.

[6] Bettinson, A.D., "The influence of constraint on creep crack growth of 316H stainless steel", Ph.D. Thesis, Mechanical Engineering Department, Imperial College London, 2002.

[7] Yatomi, M., Bettinson, A.D., O'Dowd, N.P. and Nikbin, K.M. "Modelling of damage development and failure in multiaxial notched bar creep tests", Fatigue Fract. Engng. Mater. Struct., **27**, 283–295 2004.

[8] Cocks, A.C.F. and Ashby, M.F., "Intergranular fracture during power-law creep under multiaxial stress", Metal Science, **14**, 395–402, 1980.

[9] ABAQUS version 5.8. Hibbitt, Karlsson & Sorensen, Inc., 1998.

[10] Yatomi, M, Nikbin, K.M. and O'Dowd, N.P. "Creep crack growth prediction using a damage based approach", Int. J. Press. Vess. Piping, **80**, 573–583, 2003.